Synthesis, chemical polymerization and electrochemical properties of low band gap conducting polymers for use in supercapacitors†

Patrick Soudan,[a] Philippe Lucas,[b] Hoang Ang Ho,[b] Donald Jobin,[b] Livain Breau*[b] and Daniel Bélanger*[a]

[a]Laboratoire d'Electrochimie Appliquée, Département de Chimie, Université du Québec à Montréal, Case Postale 8888, succursale Centre-Ville, Montréal, Québec, H3C 3P8, Canada. E-mail: belanger.daniel@uqam.ca; Fax: 514 987-4054; Tel: 514 987-3000 ext. 3909

[b]Laboratoire de Synthèse Organique Appliquée, Département de Chimie, Université du Québec à Montréal, Case Postale 8888, succursale Centre-Ville, Montréal, Québec, H3C 3P8, Canada. E-mail: breau.livain@uqam.ca; Fax: 514 987-4054; Tel: 514 987-3000 ext. 8788

A set of nine monomers derived from diaryl-cyanovinylene, -carboxyvinylene and -cyanobutadiene were synthesized as were the corresponding polymers resulting from the chemical polymerization of the monomers in the presence of an almost quantitative amount of $FeCl_3$ in chloroform. The aim of this work was to investigate the effect of the chemical structure of the polymers on their charge capacitance and stability upon galvanostatic charge/discharge cycling. The electrochemical performances of composite electrodes based on polymer, acetylene black and PTFE have been investigated in acetonitrile containing 1 M Et_4NBF_4 using cyclic voltammetry and galvanostatic charge/discharge cycling experiments. The best performances in terms of charge capacitance for both the p- and n-doping processes were demonstrated with poly(**7**) (2E,4E)-2,5-di-2-thienylpenta-2,4-dienenitrile and poly(**9**) (2E)-3-(2,2′-bithienyl-5-yl)-2-(2-thienyl)prop-2-enenitrile since values as high as 245 C g^{-1} were obtained with poly(**7**) in its n-doped state and 325 C g^{-1} with p-doped poly(**9**). The energy density (68 Wh kg^{-1}) and power density (24 kW kg^{-1}) delivered by a poly(**9**) capacitor are in good agreement with those expected from cyclic voltammetry and galvanostatic charge/discharge experiments performed with single electrodes. Unfortunately, a capacitance loss was observed upon cycling and was ascribed exclusively to the n-doping process occurring at the negative electrode since the capacitance of the positive electrode remained almost unchanged during these experiments.

Introduction

Many studies during the past decade have dealt with the synthesis of low band gap conducting polymers.[1] Indeed, small values for the difference in potential between the n- and p-doped states confer on these polymers enhanced stability by avoiding the problems of overoxidation or overreduction and some irreversible processes during successive potential scans.[2] Of the diverse families of monomers developed thus far to prepare low band gap polymers, we are particularly interested in the derivatives and homologues of the diaryl(cyanovinylene) family, first reported by Roncali et al.,[3] because of their potential application as active electrode materials for electrochemical supercapacitors.[4–9] In order to compare and properly evaluate the physico-chemical properties of new monomers, previously reported model compounds **1** and **2** were prepared.

The first series of new monomers shown in Chart 1 involves the replacement of one thiophene ring of **1** by dimethoxybenzene rings (**3** and **4**). The dimethoxyphenyl rings were chosen for their higher resistance toward overoxidation. In a second set, the electron-donating–withdrawing ability of substituents on the thiophene and the ethylene linkage was varied. These include a carboxylic acid in compound **5** and an electron-donating group at the 3-position of the β-thiophene ring, such as the thiophenyl group in **6**. According to Zhang

and Tour,[10] the alternating repeat of donor/acceptor units in polythiophenes favors an extended π-conjugation within the conjugated polymer backbone and contributes to a decrease of the band gap. The last series of monomers involves extending the conjugated system as this would be likely to allow for a decrease in the oxidation potential of the monomers (**7**, **8** and **9**).

The most common way used to prepare a conducting polymer involves its electrodeposition from a solution containing the monomer. Thus, poly(**1**) and poly(**2**) have been recently studied after electrodeposition on to carbon paper.[9] Nevertheless, the electrodeposition route sometimes causes problems due to the formation of soluble oligomers, leading to a lowering of the electropolymerization efficiency. Consequently and in order to use conditions closer to industrial applications, it was decided to employ polymers synthesized in the form of powders using a chemical polymerization route.[11,12] The making of the electrodes is then easier to achieve, even on a large scale, by employing a composite electrode technology comparable to that used more recently in the lithium batteries industry and for other conductive polymer-based electrochemical capacitors.[6,13–17]

Thus, in this paper we report new information concerning the electrochemical properties of chemically synthesized polymers used in composite electrodes containing 45 wt% acetylene black (AB) and 5% PTFE. In the first step, the effects of substitution patterns on the chemical polymerization yield and on the electrochemical properties of the polymers were investigated by energy dispersive analysis by X-ray (EDAX)
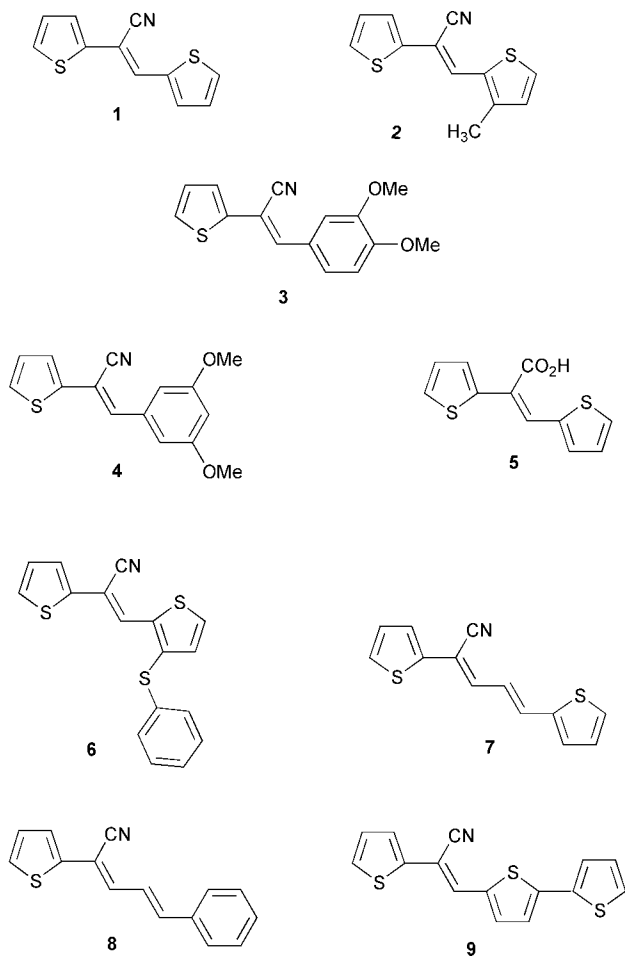

Chart 1 Structure of oligomers.

and cyclic voltammetry (CV). In the second step, the performances of the polymers as electrode materials for supercapacitors were investigated using CV and galvanostatic charge/discharge experiments and are reported together with the expected performances of the polymer-based composite electrodes in capacitor configurations. In the third step, a capacitor based on poly(**9**) was made in order to confirm the expected performances and to evaluate the cyclability of the device. Finally, and because the n-doping process was responsible for the capacitance loss of this device, the cyclability of n-doped poly(**1**), poly(**2**), poly(**7**) and poly(**9**) has been investigated up to 650 cycles and the results have been explained by considering the structure of each polymer.

Experimental section

General methods

Acetaldehyde, 2,2'-bithiophene, 3-bromothiophene, *trans*-cinnamaldehyde, 3,4- and 3,5-dimethoxybenzaldehyde, phenyl disulfide, potassium *tert*-butoxide, thiophene-2-acetic acid, thiopheneacetonitrile, thiophene-2-carboxaldehyde, 3-methylthiophene-2-carboxaldehyde and thiophenol were obtained from Aldrich Chemical Co. and were used without further purification. (2*E*)-2,3-Di-2-thienylprop-2-enoic acid **5**,[18] 3-thiophenylthiophene,[19–21] *trans*-2-(2-thienyl)acrolein[22] and 2,2'-bithiophene-5-carboxaldehyde[23,24] were prepared as previously reported. Acetylene black (AB) (Alfa, >99.9%, surface area 80 m^2 g^{-1}) was dried at 100 °C under vacuum for 12 h before use. Dry PTFE was prepared from a 60% aqueous solution after removal of water at 50 °C under vacuum and several rinses to eliminate the surfactant. Tetraethylammonium tetrafluoroborate (Et$_4$NBF$_4$) (Aldrich, 99%) was recrystallized

three times from methanol and dried under vacuum at 140 °C for 12 h prior to use. Acetonitrile (MeCN) (EM Science, Omnisolv® <10 ppm water) was used as received. Freshly activated alumina, treated at 800 °C under N$_2$ for 24 h was added to electrolytes before performing experiments in order to prevent any water contamination. Melting points were determined with a Fisher–Johns melting point apparatus and are uncorrected. Infrared spectra were recorded on a Perkin–Elmer 1600 FTIR instrument. ^{1}H NMR spectra were recorded using a Varian 300 MHz spectrometer. Chemical shifts are reported in parts per million (δ) and the signals have been designated as follows: s (singlet), d (doublet), t (triplet) and m (multiplet). ^{13}C NMR spectra were recorded at 75 MHz. Mass spectra were obtained using a GC-MS (GCD plus gas chromatography–electron ionization detector, HPG 1800A GCD system) equipped with a 5% crosslinked Ph Me silicone HP 19091 J-433 column. Separations were carried out on silica gel (7749 Merck) using circular chromatography (chromato-tron®, model 7924, Harrison Research). Elemental analyses were carried out at the Chemistry Department of the Université de Montréal on a Fisons Instrument SPA, model EA1108.

Procedure and equipment

All electrochemical experiments were performed in a glove box filled with high purity nitrogen. The electrochemical cell, filled with 1 or 2 cm^3 of electrolyte, was composed of an Ag/Ag$^+$ (10^{-2} M) reference electrode situated as close as possible to the working electrode and of a large mass (twice that of the working electrode) polymer-based composite counter electrode. In the case of the capacitor configuration, the two working electrodes were separated by a piece of Celgard® 2500. The electrochemical apparatus was composed of a potentio-stat–galvanostat Solartron model 1287 interfaced with a PC by the Corrware 2 software (Scribner Associates). Energy dispersive analysis (EDAX) was performed with a Hitachi S-5300 scanning electron microscope equipped with a Kevex Quantum 3600-0388 energy dispersive X-ray analyzer.

General procedure for the Knoevenagel condensation. (2*E*)-2,3-Di-2-thienylprop-2-enenitrile (1)[9]

To a stirred solution of thiophene-2-carboxaldehyde (2.64 g, 23.5 mmol) dissolved in ethanol (50 cm^3) was added, thio-phene-2-acetonitrile (2.90 g, 23.5 mmol), followed by potas-sium *tert*-butoxide or sodium hydroxide 10% (in mol). The formation of a yellow precipitate was observed after 10 min of stirring at room temperature. After an additional hour of stirring, the solid was filtered, washed twice with ethanol and dried, yielding 4.71 g (92%) of **1** as a yellow powder.

(2*E*)-3-[(3-methyl)-2-thienyl]-2-(2-thienyl)prop-2-enenitrile (2). Compound **2** was obtained from the Knoevenagel condensation of 3-methylthiophene-2-carboxaldehyde and thiophene-2-acetonitrile.[9]

(2*E*)-3-(3,4-Dimethoxyphenyl)-2-(2-thienyl)prop-2-enenitrile (3). Compound **3** was obtained from the Knoevenagel condensation of 3,4-dimethoxybenzaldehyde and thiophene-2-acetonitrile. Yield 78%; mp 78 °C; IR (KBr) *v*: 3099, 3086, 2997, 2217, 1602, 1591, 1508, 1273, 737 cm^{-1}; ^{1}H NMR (CDCl$_3$) δ: 3.71 (s, 3H, O-CH$_3$), 3.73 (s, 3H, O-CH$_3$), 6.7 (d, 1H), 6.84 (dd, 1H), 7.08 (m, 4H), 7.40 (d, 1H); UV (CHCl$_3$) λ_{max}: 331 nm; MS *m/z* (%): 271 (M$^+$, 100), 196 (41), 140 (11). Anal. calcd. for C$_{15}$H$_{13}$NO$_2$S: C, 66.40; H, 4.83; N, 5.16; S, 11.82. Found: C, 66.37; H, 4.88; N, 5.18; S, 11.90%.

(2*E*)-3-(3,5-Dimethoxyphenyl)-2-(2-thienyl)prop-2-enenitrile (4). Compound **4** was obtained from the Knoevenagel condensation of 3,5-dimethoxybenzaldehyde and thiophene-

2-acetonitrile. Yield 99%; IR (KBr) v: 3109, 2941, 2214, 1601, 1593, 1341, 1306, 1154, 1060, 883, 821, 731, 712 cm^{-1}; ^{1}H NMR (CDCl$_3$) δ: 3.86 (s, 6H, 2 × O-CH$_3$), 6.54 (t, J = 2.2 Hz, 1H, Ph-H4), 7.03 (dd, J = 2.2, 0.5 Hz, 2H, Ph-H2 + 6), 7.09 (dd, J = 5.2, 3.8 Hz, 1H, Th-H4), 7.32 (s, 1H, Ph-CH=), 7.33 (dd, J = 5.2, 1.2 Hz, 1H, Th-H5), 7.41 (dd, J = 3.8, 1.2 Hz, 1H, Th-H3); MS m/z (%): 271 (M$^+$, 100), 270 (29), 256 (20), 240 (23), 196 (33); ^{13}C NMR (CDCl$_3$) δ: 55.47 (2 CH$_3$), 103.29 (CH), 106.39 (C), 106.79 (2 CH), 116.79 (C), 126.27 (CH), 127.33 (CH), 128.07 (CH), 134.95 (C), 139.06 (C), 139.54 (CH), 160.91 (2 C). Anal. calcd. for C$_{15}$H$_{13}$NO$_2$S: C, 66.40; H, 4.83; N, 5.16; S, 11.82. Found: C, 66.18; H, 4.73; N, 5.15; S, 11.52%.

(2E)-2,3-Di-2-thienylprop-2-enoic acid (5)[18]. Mp 168 °C (lit. 174.5–175.5 °C); IR (KBr) v: 3390–2685 (COO$\underline{H}$), 3088, 3070, 2997, 1713 (C=O), 1663, 1599 (C=C), 1403 (weak), 1210, 1199 cm^{-1}; ^{1}H NMR (CDCl$_3$) δ: 7.05 (dd, J = 5.2, 3.6 Hz, 1H, Th-H4), 7.07 (dd, J = 4.9, 3.8 Hz, 1H, Th-H4), 7.24 (dd, J = 3.6, 1.1 Hz, 1H, Th-H3), 7.29 (dd, J = 5.2, 1.1 Hz, 1H, Th-H5), 7.35 (s, 1H, Th-C$\underline{H}$=), 7.36 (dd, J = 3.8, 1.1 Hz, 1H, Th-H3), 7.45 (dd, J = 4.9, 1.1 Hz, 1H, Th-H5); ^{13}C NMR (DMSO-d$_6$) δ: 120.73, 125.83, 126.44, 126.91, 127.73, 128.32, 129.03, 131.13, 138.00, 140.57, 169.15 (C=O); MS m/z (%): 236 (M$^+$, 100), 191 (M$^+$−CO$_2$H, 59), 147 (39), 124 (64), 113 (55), 96(33). Anal. calcd. for C$_{11}$H$_8$O$_2$S$_2$: C, 55.91; H, 3.41; S, 27.14. Found: C, 55.99; H, 3.39; S, 27.11%.

(2E)-3-[3-(Phenylsulfanyl)-2-thienyl]-2-(2-thienyl)prop-2-ene-nitrile (6). Compound **6** was obtained from the Knoevenagel condensation of 3-phenylsulfanylthiophene-2-carboxaldehyde and thiophene-2-acetonitrile. Yield 95%; mp 91 °C; IR (KBr) v: 3083, 2223, 1653, 886, 846, 823, 753, 733 cm^{-1}; ^{1}H NMR (CDCl$_3$) δ: 7.08 (m, 2H), 7.23 (m, 7H), 7.54 (d, 1H), 7.94 (s, 1H); ^{13}C NMR (CDCl$_3$) δ: 104.04, 126.41, 126.91, 126.98, 127.20, 127.34, 128.19, 128.96, 129.08, 129.26, 129.31, 129.43, 129.69, 130.29, 132.17, 136.11, 137.35; UV (CHCl$_3$) λ_{max}: 361 nm; MS m/z (%): 325 (M$^+$, 52), 215 (29), 203 (100), 172 (23). Anal. calcd. for C$_{17}$H$_{11}$NS$_3$: C, 62.74; H, 3.41; N, 4.30; S, 29.55. Found: C, 62.76; H, 3.41; N, 4.26; S, 29.47%.

(2E,4E)-2,5-Di-2-thienylpenta-2,4-dienenitrile (7). Compound **7** was obtained from the Knoevenagel condensation of *trans*-2-(2-thienyl)acrolein and thiophene-2-acetonitrile. Yield 52%; mp 92 °C; IR (KBr) v: 3094, 2218, 1597, 1419, 956, 845, 723, 705 cm^{-1}; ^{1}H NMR (CDCl$_3$) δ: 7.04–7.14 (m, 5H), 7.20 (dd, J = 3.6, 1.0 Hz, 1H), 7.28–7.32 (m, 2H), 7.36 (dd, J = 5.0, 1.0 Hz, 1H); UV (CHCl$_3$) λ_{max}: 389 nm; MS m/z (%): 243 (M$^+$, 100), 210 (27), 159 (25), 245 (10). Anal. calcd. for C$_{13}$H$_9$NS$_2$: C, 64.16; H, 3.73; N, 5.76; S, 26.35. Found: C, 63.95; H, 3.76; N, 5.84; S, 26.57%.

(2E,4E)-5-Phenyl-2-(2-thienyl)penta-2,4-dienenitrile (8). Compound **8** was obtained from the Knoevenagel condensation of *trans*-cinnamaldehyde and thiophene-2-acetonitrile. Yield 80%; mp 98 °C; IR (KBr) v: 3098, 3021, 2208, 1605, 1447, 1320, 965, 843, 753, 707, 687 cm^{-1}; ^{1}H NMR (CDCl$_3$) δ: 7.00 (dd, J = 16.0 Hz, 1H), 7.07 (dd, J = 5.1, 3.8 Hz, 1H), 7.21 (d, J = 16.0 Hz, 1H), 7.26–7.44 (m, 6H), 7.55 (dd, J = 8.8, 2.6 Hz, 2H); UV (CHCl$_3$) λ_{max}: 367 nm; MS m/z (%): 237 (M$^+$, 100), 115 (49), 160 (40), 91 (26). Anal. calcd. for C$_{15}$H$_{11}$NS: C, 75.91; H, 4.67; N, 5.90; S, 13.51. Found: C, 75.65; H, 4.67; N, 5.88; S, 13.77%.

(2E)-3-(2,2′-Bithienyl-5-yl)-2-(2-thienyl)prop-2-enenitrile (9). Compound **9** was obtained from the Knoevenagel condensation of 2,2′-bithiophene-5-carboxaldehyde and thiophene-2-acetonitrile. Yield 91%; mp 110 °C; IR (KBr) v: 3106, 3023, 2212, 1572, 1444, 1250, 910, 841, 703, 680 cm^{-1}; ^{1}H NMR (CDCl$_3$) δ: 7.06 (m, 2H), 7.17 (d, 1H), 7.30 (m, 4H), 7.40 (s, 1H), 7.44 (d, 1H); ^{13}C NMR (CDCl$_3$) δ: 102.42, 117.27, 124.20,

125.42, 126.10, 126.27, 127.01, 128.44, 130.39, 132.06, 133.95, 136.28, 136.60, 139.09, 142.23; UV (CHCl$_3$) λ_{max}: 409 nm; MS m/z (%): 299 (M$^+$, 100), 127 (25), 149 (12), 109 (10). Anal. calcd. for C$_{15}$H$_9$NS$_3$: C, 60.17; H, 3.03; N, 4.68; S, 32.12. Found: C, 60.21; H, 2.97; N, 4.58; S, 32.04%.

Chemical polymerization

Polymers were prepared by chemical oxidation of the monomers using iron trichloride according to a procedure similar to that of Sugimoto *et al.*[11] Note that the procedure described below for poly(**1**) was used for the other polymers on various scales with the exception that the quantity of FeCl$_3$ was lowered to 1.8 equivalents in each case to avoid chlorination of the polymer.

Poly[(2E)-2,3-di-2-thienylprop-2-enenitrile] [poly(1)]

To a solution of iron trichloride (0.74 g, 4.6 mmol, 2 eq.) in chloroform (20 cm^3) under nitrogen was added dropwise a solution of the monomer **1** (0.50 g, 2.3 mmol, 1 eq.) in 10 cm^3 of chloroform. The mixture was heated under reflux for a period of 8 h and was then stirred at room temperature for an additional 16 h. The mixture was poured in methanol (150 cm^3). The black precipitate was collected on a sintered glass funnel and washed with methanol (3 × 50 cm^3). The polymer was then washed by Soxhlet extraction using methanol for a 24 h period and dried under reduced pressure at 50 °C for 1 h to yield 0.35 g (yield 70%) of poly(**1**).

Preparation of the composite electrodes

Polymer powder (typically 20–50 mg) was first ground with acetylene black in an agate mortar. The mixture was then placed in a small beaker, dry PTFE was added and the components were mixed in the presence of pure ethanol until a rubbery paste was obtained. Finally, several successive rolling and foldings with ethanol on a glass plate resulted in a thin film (around 5 mg cm^{-2}) with good mechanical properties. After drying under vacuum at 50 °C, which removes the ethanol, the film was approximately composed of 50% polymer, 45% AB and 5% PTFE. To ensure good electrical contact between the components of the mixture and to increase the solidity of the resulting electrodes, the film was pressed between two aluminium grids under a pressure of about 500 MPa cm^{-2}. The size of the composite electrodes, including the metallic support, was generally close to 0.5 cm^2 but the geometric area of the enclosed polymer film varied significantly, as did its mass. Therefore, all the results have been reported with respect to the mass of the active polymer present in the electrodes.

Results and discussion

Synthesis of monomers

All of the monomers, with the exception of compound **5**, were prepared by a Knoevenagel condensation reaction between thiophene-2-acetonitrile and the appropriate aryl aldehyde in the presence of the base potassium *tert*-butoxide as reported by Roncali *et al.*[3] This condensation exclusively provides the *trans*-isomer,[25] which allowed us to obtain a large number of pure new monomers on a large scale and in suitable purity for physico-chemical studies. Monomer **5** was obtained by a Perkin condensation between thiophene-2-carboxaldehyde and thio-phene-2-acetic acid as a mixture of *cis*- and *trans*-isomers. These isomers can be obtained in pure form by crystal-lization.[18] The synthesis of monomer **6** involved initial preparation of 3-thiophenylthiophene by the nucleophilic substitution reaction of thiophenolate with 3-bromothiophene in the presence of a catalyst such as CuI, CuO or Cu$_2$O.[19,20] This reaction furnished a final product contaminated with

several secondary products. We were unable to purify this product by distillation or by chromatography on silica. In all cases, the crude product was contaminated with varying amounts of phenyl disulfide detected by GC-MS. Alternatively, the method described by Wu et al.[21] was used. 3-Lithiothiophene was treated with phenyl disulfide in a mixture of solvents (hexane–THF, 10:1). The formylation of 3-thiophenylthiophene and subsequent Knoevenagel condensation of the corresponding 2-formyl derivative was then carried out as described above. The preparation of trans-2-(2-thienyl)acrolein, which is required to prepare monomer 7, has been described by Klemm and Gopinath.[22] It involves the addition of thiophene-2-carboxaldehyde to an alkaline solution of acetaldehyde.

EDAX characterization of the polymers

EDAX was used to determine the residual Fe and Cl content of the polymers, since some $FeCl_3$, $FeCl_2$ or related anions such as $FeCl_4^-$ could be adsorbed on the polymer. In some cases, iron or chlorine could be incorporated into the polymer in the form of chlorinated polymers[17] or iron complexes of the polymers.[12,26] The results presented in Table 1 show that the Fe and Cl content can vary significantly from one polymer to another.

Firstly, low Cl and Fe contents were found for poly(1), poly(2), poly(7), poly(8) and poly(9) and contribute no more than 3% to the mass of the resulting polymers. In addition, the Cl content is about 2 to 3 times higher than the Fe content. These data are consistent with species such as $FeCl_2$ or $FeCl_3$ adsorbed at the polymer surfaces. Since the polymers are obtained in their undoped form after washing with hot methanol (Soxhlet extraction), the presence of doping anions such as Cl^- or $FeCl_4^-$ is unlikely. We also notice that the polymerization yields for poly(1), poly(2), poly(7) and poly(9) are rather satisfactory and found to be between 55 and 70%, whereas those of poly(3), poly(4), poly(6) and poly(8) are fairly low (less than 20%). The lower polymerization yield of poly(2) (55%) relative to that of poly(1) (70%) can be explained by the presence of the additional methyl group, which is known to have deleterious consequences on the electropolymerization efficiency.[1b,3,9] Table 1 also shows that poly(7) and poly(9), derived from related monomers, have similar polymerization yields ($\sim 65\%$). The low polymerization yield of poly(8) (10%) can be explained by the particular molecular structure of monomer 8, which contains only one 2-position available on the thiophene unit for the polymerization, and by the fact that the oxidation of the phenyl unit requires a higher potential than that of thiophene. Thus, the reaction products may predominantly consist of small oligomers. Moreover, the low polymerization yield for poly(8) is in agreement with the lack of electrochemical polymerization observed for an analogous oligomer that contains only one cyanoethylene between a thiophene and a phenyl ring.[27] The same reason can be invoked to explain the lack and low (20%) polymerization yield of

poly(3) and poly(4), respectively since the corresponding monomers also have only one thiophene 2-position available. On the other hand, electroactive polymers have been recently generated from compounds possessing one thiophene and one dimethoxybenzene ring linked together by either a cyanoethylene[27b] or a polyether chain.[28] However, in our hands the chemical polymerization is inhibited in the presence of 2-methoxy substituents in meta- and para-positions (monomer 3) whereas the polymerization occurs for the meta-isomer (monomer 4), presumably at the para- and 2-positions of the phenyl and thiophene rings, respectively. Possible structures for the corresponding polymers are presented in Scheme S1 of the electronic supplementary data.

Secondly, the chlorine content of poly(6) and especially of poly(4) is particularly high and is respectively 7 and 50 times higher than their corresponding Fe content, indicating that some chlorine has been incorporated into the structure of the polymer during the polymerization process. Indeed, for poly(6), the Cl content is about 0.4 Cl atom per monomer unit. Thus, the major part of these chlorine atoms might be covalently linked to the polymer. Indeed, it has been previously demonstrated that certain positions of polythiophene derivatives can be involved in the electrochemical oxidative substitution of H atoms by Cl atoms, leading to chlorinated polymers.[29–32] Furthermore, chlorinated poly(1) and poly(2) were recently obtained by our group[16,17] by chemical polymerization of the monomers by a procedure similar to that used in the present work, which involves a large excess (6 equivalents) of $FeCl_3$ as oxidant. Thus, poly(6) presumably contains some covalently bonded chlorine resulting from the oxidative substitution of H atoms by Cl atoms at the 3- and 4-positions (in the presence of Fe^{3+} as oxidative agent and Cl^- as nucleophile) or eventually elsewhere on the ethylene linkage or on the phenyl ring. We can postulate that the thiophenyl group in poly(6) is responsible for the chlorination of this polymer, since similar polymers, in particular poly(1) and poly(2), are not chlorinated when low oxidant concentration is used as is the case in this work. Nevertheless, the chlorine content of poly(6) increases the mass of the polymer by about 5–6% relative to the non-chlorinated polymer. On the other hand, the low polymerization yield (10%) of poly(6) can possibly be ascribed to the steric hindrance of the thiophenyl group. In the case of poly(4), the Cl content reaches 0.75 Cl atom per monomer unit, leading to an increase of its apparent molecular weight by about 10%. An explanation of this high degree of Cl substitution could be the different molecular structure of monomer 4 in comparison with the others. This could be due on one hand to the presence of only one available 2-position on the thiophene ring, which would lead to complications during the polymerization process and to a polymer with a different reactivity towards Cl substitution. In addition, the presence of two methoxy groups in meta-positions of the phenyl ring might induce an activation of the para-position towards Fe^{3+} oxidation followed by substitution with Cl^-. Nevertheless,

Table 1 Characteristics of the chemically synthesized polymers

| Polymer	Theoretical formula	Theoretical molecular weight/g mol^{-1a}	Yield (%)^b	Fe:S atomic ratio from EDAX	Cl:S atomic ratio from EDAX	Experimental formula^c	Experimental molecular weight/g mol$^{-1})^a$
1	$(C_{11}H_5NS_2)_n$	215.3	70	<0.01	0.03	$(C_{11}H_5NS_2Cl_{0.06})_n$	217
2	$(C_{12}H_7NS_2)_n$	229.3	55	<0.01	0.04	$(C_{12}H_7NS_2Cl_{0.08})_n$	232
3	$(C_{15}H_{11}NO_2S)_n$	269.3	0	—	—	—	—
4	$(C_{15}H_{11}NO_2S)_n$	269.3	20	0.01	0.75	$(C_{15}H_{11}NO_2SCl_{0.75})_n$	296
5	$(C_{11}H_6O_2S_2)_n$	234.3	90	0.16	0.04	$(C_{11}H_6O_2S_2Fe_{0.32}Cl_{0.08})_n$	255
6	$(C_{17}H_9NS_3)_n$	323.4	10	0.02	0.14	$(C_{17}H_9NS_3Fe_{0.06}Cl_{0.42})_n$	342
7	$(C_{13}H_7NS_2)_n$	241.3	65	<0.01	0.02	$(C_{13}H_7NS_2Cl_{0.04})_n$	243
8	$(C_{15}H_9NS)_n$	235.3	10	0.04	0.08	$(C_{15}H_9NSFe_{0.04}Cl_{0.08})_n$	241
9	$(C_{15}H_7NS_3)_n$	297.4	65	0.01	0.02	$(C_{15}H_7NS_3Fe_{0.03}Cl_{0.06})_n$	301

^{a}Related to the monomer unit in the polymer. ^{b}Yield = isolated product mass:monomer mass. ^{c}Deduced from EDAX.

additional work by a technique such as X-ray photoelectron spectroscopy would be required to determine the electronic properties of the chlorine atoms (*e.g.* covalently bonded or free chloride ions).

Thirdly, and in contrast to the other polymers, the Fe content of poly(**5**) is higher than that of Cl by a factor of 4, indicating that iron cations are incorporated into the polymer without the presence of chloride anions. Thus, we can postulate that the counterions of these iron cations (about 0.32 Fe atom per monomer unit) are the carboxylate anions (CO_2^-) resulting from the deprotonation of the acidic CO_2H functionalities. This hypothesis is in good agreement with the CO_2^- : Fe ratio, which is close to 3, if the cations are Fe^{3+}. Nevertheless, a more likely possibility involves Fe^{2+} cations (derived from the reduction of Fe^{3+}) linked to two carboxylate anions, while one carboxylic group remains protonated. Evidence for the predominance of the carboxylate form was obtained from IR spectroscopy. Absorption bands at 1676 (broad, CO_2H) and 1600 cm^{-1} (weak, C=C) were observed for an electrogenerated poly(**5**) (on to a Pt plate from a dichloromethane solution) in Nujol. These are in good agreement with the free carboxylic stretch of monomer **5**, which is observed at 1713 cm^{-1} (strong absorption band, CO_2H) and the C=C stretch at 1599 cm^{-1}. However, the chemically generated polymer showed the following absorption bands in Nujol; 1604 (strong) and 1389 cm^{-1} (strong). These are consistent with the corresponding sodium carboxylate salt of the monomer **5**, which shows an asymmetric stretch for the carboxylate group at 1597 cm^{-1} (strong, CO_2^- and C=C) and a symmetric stretch at 1441 cm^{-1} (strong, CO_2^-). A weak absorption band at 1692 cm^{-1} was also present for the chemically generated polymer, which is attributed to some free carboxylic acid groups. Also, the molecular weight is increased by about 9% because of the Fe content, leading to an overestimation of the polymerization yield, which reached 90%. The presence of Fe in poly(**5**) is in contradiction to a previous report on self-doped poly-3-(ω-carboxyalkyl)thiophenes and for which the carboxylate groups were predominantly in their undissociated form.[33] In addition, it will be shown later that the presence of iron has deleterious consequences on the electrochemical behavior of poly(**5**).

Cyclic voltammetry of the polymers

Composite electrodes of mass varying between 0.5 to 2 mg and containing 50% polymer were used. The chemically synthesized polymers were characterized by cyclic voltammetry (CV), the results of which are presented in Figs. 1 and 2 for the polymers of **1**, **2**, **4**, **5**, **6**, **7** and **9**. Relevant parameters extracted from the CV data are also summarized in Table 2. It should be noticed that monomers with only one thiophene ring either cannot be chemically polymerized (monomer **3**) or form corresponding polymers that show poor and ill-defined electrochemistry and
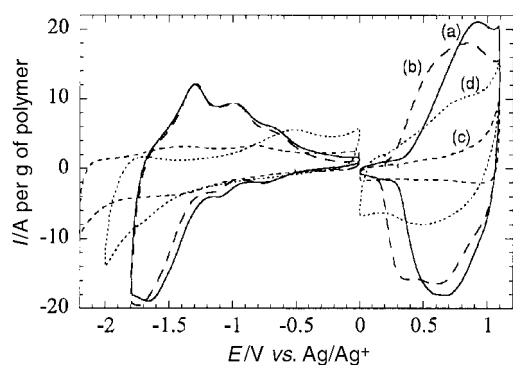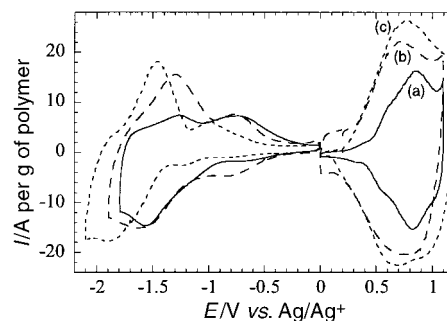
Fig. 2 Cyclic voltammograms of composite electrodes based on (a) poly(**6**) (solid line), (b) poly(**7**) (broken line) and (c) poly(**9**) (dashed line) in 1 M Et_4NBF_4–acetonitrile. Scan rate: 50 mV s^{-1}.

low charge storage capacity (polymer of compound **4**). As a representative example, the CV of poly(**4**) shown in Fig. 1 translates into charge capacities of 36 and 105 C g^{-1} for the p- and n-doping states, respectively. These values include the contribution of acetylene black used for the fabrication of the composite electrode, which amounts to 10 F g^{-1} of the electrode capacitance.[16,17]

The CV of poly(**5**) exhibits enhanced electroactivity for the p-doping process relative to poly(**4**) with a charge capacity for p-doping of 130 C g^{-1} ring whereas that for the n-doping is smaller and limited to 70 C g^{-1}. The potential for the p-doping process cannot be precisely determined since the oxidative and reductive redox reactions take place over a large potential window between 0 and 1.1 V. In addition, the CV is asymmetric and irreversible since the p-doping process occurs at notably higher potential than the p-dedoping one. The significant polarization observed when the potential is reversed is not due to the solution uncompensated resistance, which is smaller than 1 Ω, but rather to the internal impedance of the working electrode. The low conductivity of the polymer can be rationalized when one considers its chemical composition. Indeed, poly(**5**) is an iron complex (*vide supra*), which is probably incompatible with long polymeric chains and consequently with the high delocalization of π-electrons necessary to ensure a high conductivity. So, the presence of iron in this polymer appears to have deleterious consequences on its electrochemical behavior. Thus, another polymerization process must be developed such as electropolymerization or the use of another oxidant such as $NOBF_4$, which has already been used for the chemical polymerization of some monomers.[5a,34] in order to avoid the formation of iron complexes and to obtain an iron-free polymer.

The CV of poly(**1**) shows p- and n-doping processes centered around 0.9 and −1.65 (main wave) V, respectively. Although the n-doping/dedoping is clearly better defined than in the cases of poly(**4**) and poly(**5**), the redox process is not perfectly reversible. This asymmetry indicates that the n-doping process is more problematic than the p-doping one, as has been previously reported by several authors,[2a,35] in particular by Zotti and Schiavon[36] who noticed that the n-doping/dedoping wave of poly(dithienylethylene) is well defined only for very thin films. In contrast to poly(**4**) and poly(**5**), the p- and n-doping charge capacities of poly(**1**) are similar and values of 210 and 200 C g^{-1} were found, respectively. These values are close to those obtained with electrochemically synthesized PFPT.[32,37,38]

The predictable effect of an electron-donating group in poly(**2**) is a lowering of the p-doping potential due to stabilization of the positively charged p-doped polymer. The CV of poly(**2**), presented in Fig. 1, resembles that of poly(**1**), with the exception of a displacement of the p- and n-doping waves towards less positive potential by about 0.1 V, which is in good agreement with the predicted effect of the methyl group and a slight increase in the p-doping charge capacity [230 *vs.*

Fig. 1 Cyclic voltammograms of composite electrodes based on (a) poly(**1**) (solid line), (b) poly(**2**) (broken line), (c) poly(**4**) (dashed line) and (d) poly(**5**) (dotted line) in 1 M Et_4NBF_4–acetonitrile. Scan rate: 50 mV s^{-1}.

Table 2 Electrochemical properties of the chemically synthesized polymers

Polymer	Potential of p-doping and *dedoping*/V *vs.* Ag/Ag$^+$	Specific capacitance in the p-doped state/C g^{-1}	Potential of n-doping and *dedoping*[a]/V *vs.* Ag/Ag$^+$	Specific capacitance in the n-doped state/C g^{-1}
1	0.9	210	−1.65	200
	0.7		*−1.3/−1*	
2	0.8	230	−1.75	185
	0.6		*−1.3/−1*	
4	Ill defined	36	Ill defined	105
5	Ill defined	130	Ill defined	70
6	0.85	150	−1.55	185
	0.85		*−1.25/−0.75*	
7	0.7	275	−1.65	245
	0.7		*−1.3*	
9	0.75	325	−1.85	220
	0.75		*−1.45*	

[a]Potential of the main waves.

210 C g^{-1} for poly(**1**)]. This increase of capacitance can be ascribed to the stabilizing effect of the methyl group on the positively charged p-doped polymer and also to the lowering of the potential of the p-doping process, which is then more complete at 1.1 V. On the other hand, the shape of the CV of poly(**2**) is very similar to that reported by Zotti and Schiavon[36] for a poly(dithienylethylene) thin film electrodeposited on to Pt, since the p-dedoping process is located on a wider potential range than the p-doping process. The charge capacitance of poly(**2**) is slightly lower compared to that of poly(**1**) (185 *vs.* 200 C g^{-1}) due to the higher molecular weight of its monomer unit.

The CV of poly(**6**), shown in Fig. 2, exhibits p- and n-doping waves centered at 0.85 and −1.55 V, respectively. The p-doping/dedoping process of poly(**6**) appears to be more reversible than that of poly(**1**) and poly(**2**) whereas the opposite is true for the n-doping process. The electron donating effect of the thiophenyl group seems to be verified since the p-doping wave of poly(**6**) appears at a 50 mV less positive potential than for the non-substituted poly(**1**). Nevertheless, the effect is not confirmed if one considers the p-dedoping potential or the n-doping potential (see Table 2), which are more positive than the corresponding values of poly(**1**). Thus, if these two latter values are considered, the p-doped state of poly(**6**) appears to be destabilized (*i.e.* occurs at higher potential values) in comparison with poly(**1**) and accordingly the n-doped state of poly(**6**) is stabilized (*e.g.* occurs at less negative potential values). This is possibly due to the presence of 0.1–0.2 Cl atom per thiophene ring (*vide supra*), which can act as an electron-withdrawing group and then destabilize the positively charged p-doped polymer or stabilize the n-doped state. The specific capacitance for p-doping of poly(**6**) is limited to 150 C g^{-1} owing to the higher molecular weight of its monomer unit in comparison with the two latter. On the other hand, the specific capacitance for n-doping of poly(**6**) (185 C g^{-1}) is equal to that of poly(**2**) and smaller than that of poly(**1**) owing to the higher molecular weight of monomer **6**. Finally, it is worth noting that the Cl content in poly(**6**) does not appear to have harmful consequences on the doping processes.

The polymer **7** is relatively different from the preceding ones since it contains an additional ethylene group to the ethylene linkage of poly(**1**). The CV of poly(**7**), reproduced in Fig. 2, exhibits a well-defined and reversible redox wave centered at 0.7 V as well as a main n-doping wave at −1.65 V and the corresponding dedoping wave at −1.3 V. One can also notice the presence of a secondary redox process at −0.8 V. The specific current is notably higher than for poly(**6**), leading to specific capacitances of 275 and 245 C g^{-1} for the p- and n-doping processes, respectively. The latter are the highest values for n-doping of all the polymers investigated here and are particularly high values for a polythiophene derivative. For

instance, these values are more than 40% higher than that of poly(**1**). Therefore, the additional ethylene group appears to be very beneficial for the p-doping process. This is also confirmed by a 0.2 V decrease of the p-doping potential of poly(**7**) in comparison with poly(**1**). These results are in good agreement with the expected effect of an additional ethylene group to extend the conjugated system and thus lower the oxidation potential of the polymer.[1a,39,40]

The last polymer, poly(**9**), differs from poly(**1**) by the addition of a supplementary thiophene ring. The CV of poly(**9**), depicted in Fig. 2, is similar to that of poly(**7**), with the exception that i) the p-doping potential is more positive by about 50 mV, ii) the maximum specific current is slightly higher and iii) the oxidation limit is extended up to 1.2 V. The CV of poly(**9**) also exhibits a cathodic wave at −1.85 V and its anodic counterpart at −1.45 V. Thus, the n-doping process resembles that of poly(**7**) with the exception of a 200 mV shift of the redox wave towards more negative values and also a slightly higher specific current. The specific capacitance (325 C g^{-1}) for p-doping of poly(**9**) is the highest for the polymers investigated here. On the other hand, the specific capacitance for n-doping of poly(**9**) is only 10% lower than that of poly(**7**) owing to the lower molecular weight of monomer **9** and attains 220 C g^{-1}. Thus, the extension of the conjugated system, achieved with either an additional ethylene or a thiophene group, appears to improve the performance of these polythiophene derivatives. Finally, poly(**9**) appears to be the polymer that undergoes the n-doping process at a more negative value (−1.85 V), and is also the one that can be p-doped up to higher potential (1.2 V). Consequently, poly(**9**) presents the widest voltage difference between its p- and n-doped states (Table 3) and hence is the polymer with the highest band gap. The explanation probably lies in the presence of a bithiophene unit in the monomer, which leads to a polymer with longer polythiophene sequences (up to 4 thiophene rings linked together, see Scheme S1 of the supplementary information) and resembles poly(bithiophene), which is n-doped at extremely negative potentials (< −2.1 V).[2a,13]

Effect of the scan rate

The polymers of **1**, **2**, **6**, **7** and **9** are characterized by high values of specific capacitances both in their p- and n-doped states, when a scan rate of 50 mV s^{-1} is used in cyclic voltammetry, which could lead to high specific energy for a supercapacitor assembled from these polymers. This scan rate corresponds approximately to discharge times of about 10–40 s depending on the potential windows that are compatible with supercapacitor applications. Nevertheless, the polymers were tested under higher scan rates, up to 500 mV s^{-1}, in order to evaluate the kinetic limitations of the doping processes, and also the capabilities of the composite electrodes to deliver high power

Table 3 Expected performance of the polymers in capacitor configurations
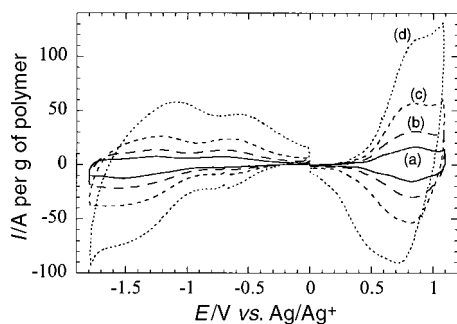
Polymer	Mean n-dedoping potential/V[a]	Specific n-doping capacitance/C g^{-1a}	Mean p- and n-voltage difference/V[b]	Specific capacitance of a capacitor/C g^{-1c}	Specific energy of a capacitor/W h kg^{-1d}	Specific power of a capacitor/kW kg^{-1e}
1	−1.1	180	1.8	97	49	18
2	−1.1	175	1.7	99	47	17
6	−1.1	150	1.9	75	40	14.5
7	−1.2	240	1.9	128	68	24.5
9	−1.35	210	2.1	128	75	27
9 (+)	—	—	1.95	138	75	27
7 (−)	−1.2	240				

[a]Deduced from galvanostatic discharge curves. [b]Difference between mean p- and n-dedoping potentials. [c]Calculated from the charge and mass of polymer in an assembly of a positive (p-doped) and a negative (n-doped) electrodes. [d]Calculated from the specific capacitance and the mean p- and n-voltage difference. [e]Calculated from the specific energy and a discharge time of 10 s.

densities. As a representative example, Fig. 3 presents the CVs of a poly(**6**)-based composite electrode recorded at a scan rate of between 50 and 500 mV s^{-1} for both the p- and n-doped redox processes. A 27% decrease of the capacitance is found between 50 and 500 mV s^{-1} but nonetheless a very high power density can be achieved since a scan rate of 500 mV s^{-1} corresponds to a discharge time of 2 s. On the other hand, it is interesting to note that the peak potentials for the p- and n-doping waves do not change up to 200 mV s^{-1} but at a higher scan rate of 500 mV s^{-1} the shape of the CVs is modified and the polarization becomes significant. This corresponds to the upper limit that can be tolerated by the electrodes while maintaining small polarization loss. The effect of scan rate on the electrochemical behavior of the polymers is reported in Fig. 4 for the polymers displaying the highest charge capacities. Nevertheless, the scan rate was limited to 200 mV s^{-1} for all the polymers but poly(**6**) since this scan rate corresponds to the typical faster switching time (10 s) needed for most supercapacitor applications. It can be seen that the capacitance loss is slightly more important for the n-doping process than for the p-doping one when the scan rate is increased, but the difference is not very significant. This is somewhat surprising since the ?tjl=0>n-doping process is usually less reversible and slower than the p-doping one. On the other hand, Fig. 4 also shows that poly(**6**) is less sensitive to the increase of the scan rate than the other polymers. For this series of polymers, the capacitance loss of between 50 and 200 mV s^{-1} follows the order of poly(**6**) < poly(**1**) = poly(**2**) < poly(**7**) < poly(**9**). In spite of this, the capacitance loss for poly(**9**) is limited to about 10% at 100 mV s^{-1} and to 30% at 200 mV s^{-1}, which are still acceptable values.

Performance of the polymers in single electrodes and in supercapacitor-type configuration

In order to complete the voltammetric study and to get some insight into the behavior of the polymers in capacitor configuration, the com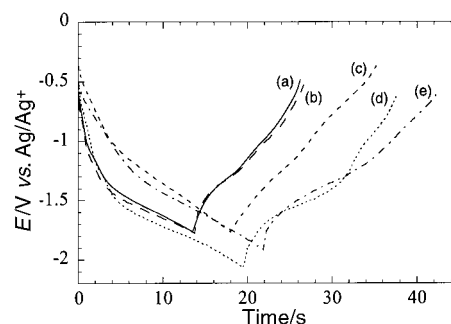posite electrodes were tested under galvanostatic charge/discharge cycling. Only the polymers exhibiting the most promising cyclic voltammetric performance were evaluated. Fig. 5 presents single electrode charge/discharge curves of selected polymers for the n-doping redox process. The shapes of these curves differ from that expected for ideal capacitive behavior (*e.g.* linear variation with time) that was obtained for the p-doped process (not shown).

The discharge curves were used to estimate the mean n-dedoping voltage for each polymer, as well as their specific capacitance, specific energy and specific power in capacitor configuration, which are reported in Table 3. The data allow a reasonable estimation of the expected performance of a supercapacitor assembled with a positive electrode (*i.e.* p-doped) and a negative polymer electrode (*i.e.* n-doped). The resulting performances are in good agreement with the
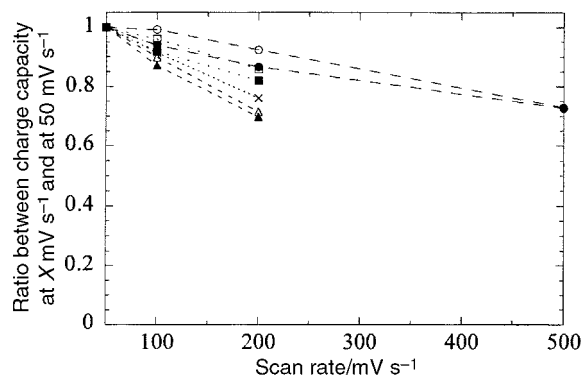
Fig. 4 Ratios of the charge capacitance at a scan rate X and at a scan rate of 500 mV s^{-1} as a function of the scan rate X during cyclic voltammetry of composite electrodes based on (■) n-doped poly(**1**), (□) p-doped poly(**2**), (●) n-doped poly(**6**), (○) p-doped poly(**6**), (▼) n-doped poly(**7**), (×) p-doped poly(**7**), (▲) n-doped poly(**9**) and (△) p-doped poly(**9**) in 1 M Et$_4$NBF$_4$–acetonitrile.

Fig. 3 Cyclic voltammograms of composite electrodes based on (a) poly(**6**) in 1 M Et$_4$NBF$_4$–acetonitrile at scan rates of (a) 50, (b) 100, (c) 200 and (d) 500 mV s^{-1}. Left: potential window 0/−1.8 V. Right: potential window 0/+1.1 V.
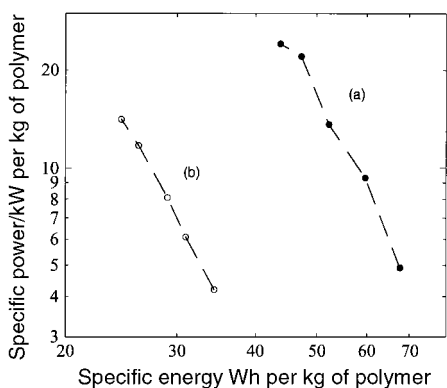
Fig. 5 Galvanostatic charge/discharge cycles of composite electrodes based on (a) poly(**1**) (solid line), (b) poly(**2**) (broken line), (c) poly(**6**) (dashed line), (d) poly(**7**) (dot–dashed line) and (e) poly(**9**) (dotted line) in their n-doped state in 1 M Et$_4$NBF$_4$–acetonitrile. Specific currents (A g^{-1} of polymer): poly(**1**) 12.9, poly(**2**) 12.1, poly(**6**) 8.4, poly(**7**) and poly(**9**) 10.5.
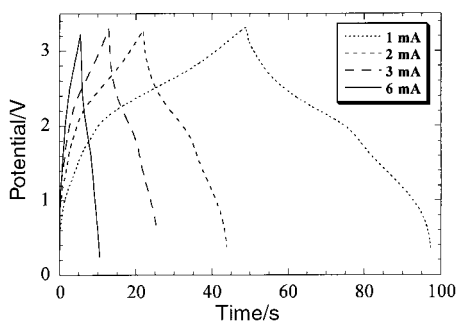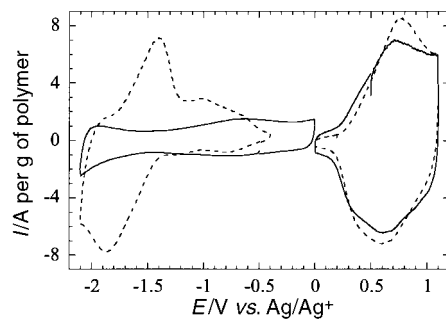
Fig. 6 Galvanostatic charge/discharge cycles of a capacitor composed of poly(**9**)-based composite electrodes (positive electrode: 0.17 mg of poly(**9**); negative electrode: 0.23 mg of poly(**9**)) and recorded between 0.3 and 3.1 V in 1 M Et$_4$NBF$_4$–acetonitrile under currents varying from 1 to 6 mA.
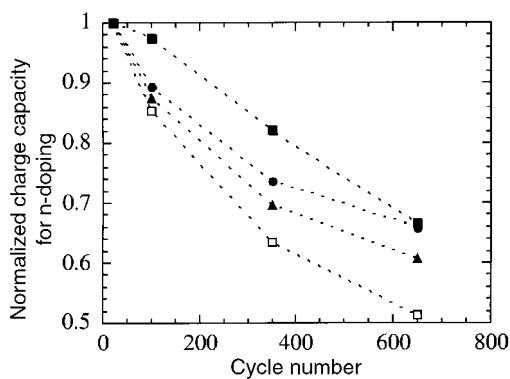

Fig. 8 Cyclic voltammograms of poly(**9**)-based electrodes comprising a capacitor based on this polymer (see caption of Fig. 7) recorded in 1 M Et$_4$NBF$_4$–acetonitrile at a scan rate of 20 mV s^{-1} at the beginning (cycle 20, dashed line) and at the end (cycle 1300, solid line) of the cycling experiment. Left: negative (n-doped) electrode; right: positive (p-doped) electrode.

results obtained from the cyclic voltammetric studies, since the lower performances are achieved with poly(**6**), whereas higher performances are obtained with poly(**7**) and poly(**9**) due to their higher doping levels and lower molecular weight per thiophene unit. Indeed, the maximum specific capacitance of 128 C g^{-1} is obtained for these two polymers and the maximum specific energy of 75 Wh kg^{-1} and specific power of 27 kW kg^{-1} (for a discharge time of 10 s) are obtained with poly(**9**). These values, in particular the value of the specific energy, are among the highest ever reported in the literature for conductive polymers.[37c,41] On the other hand, poly(**7**) exhibits a higher specific capacitance upon n-doping than poly(**9**), while the latter is characterized by a slightly higher specific capacitance upon p-doping than poly(**7**). Thus, a super-capacitor based on a poly(**9**) positive electrode and on a poly(**7**) negative electrode was considered and the expected performances of the resulting capacitor are given at the end of the Table 3. This asymmetric assembly allows a higher specific capacitance (138 C g^{-1}) than symmetrical poly(**7**)- or poly(**9**)-based capacitors, but unfortunately no increase is obtained in terms of specific energy and specific power in comparison with a poly(**9**)-based capacitor.

In order to validate these expectations and to evaluate the cyclability of the polymer, a capacitor composed of two poly(**9**)-based composite electrodes was assembled. This capacitor was cycled galvanostatically at currents ranging from 1 to 6 mA (Fig. 6) and as expected the mean discharge voltage and the specific energy decreased with an increase of the discharge current (see Table S2, supplementary information). A maximum specific energy of 68 Wh kg^{-1} is reached under a current of 1 mA, while the maximum specific power (24 kW kg^{-1} of polymer) is attained when the current is

equal to 6 mA. Thus, these values are very close to those expected from single electrode measurements (*i.e.* 75 Wh kg^{-1} and 27 kW kg^{-1}) and demonstrate that capacitor performance can be estimated properly from the CV and single electrode charge/discharge data. The galvanostatic charge/discharge cycling experiment was completed under a constant current of 2 mA and a substantial capacitance loss of 45% was observed between cycles 100 and 1 300. This deterioration of the performance is illustrated by the Ragone plots in Fig. 7.

In order to better understand the origin of this capacitance decay, cyclic voltammograms of poly(**9**) electrodes were recorded separately on both electrodes of the capacitor at the beginning and at the end of the cycling and are depicted in Fig. 8. These CVs clearly illustrate that the capacitance loss is exclusively due to the degradation of the negative electrode, since the coulombic charge corresponding to its CVs recorded between 0 and −2.1 V is lowered by 47%, while the charge of the CVs of the positive (p-doped) electrode is lowered by only 0.3%. Thus, the cyclability of poly(**9**) is very high in its p-doped state, but it is not so in its n-doped state.

Cyclability of the polymers in their n-doped state

In order to determine whether or not the capacitance fading of poly(**9**) upon cycling in its n-doped state is also observed with other polymers, and since a good cyclability is required for a supercapacitor, cycling experiments were performed using a discharge time of about 10 s on single electrodes composed of polymers of **1**, **2**, **7** and **9** in their n-doped state. The plot of the normalized charge capacitance for n-doping as a function of the cycle number up to 650 cycles for each polymer contained in these electrodes is shown in Fig. 9. Evidently, an appreciable

Fig. 7 Ragone plots for a capacitor composed of poly(**9**)-based composite electrodes (positive electrode: 0.17 mg of poly(**9**); negative electrode: 0.23 mg of poly(**9**)) cycled between 0.3 and 3.1 V in 1 M Et$_4$NBF$_4$–acetonitrile. (a) After 50 cycles and (b) after 1 400 cycles.

Fig. 9 Evolution of the normalized charge capacity for n-doping of polymer composite electrodes based on (■) poly(**1**), (□) poly(**2**), (▲) poly(**7**) and (●) poly(**9**) as a function of the number of cycles in their n-doped state with a discharge time of about 10 s. Electrolyte: 1 M Et$_4$NBF$_4$–acetonitrile.
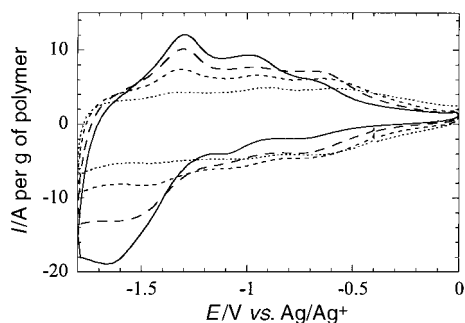
Fig. 10 Cyclic voltammograms of poly(**1**)-based composite electrode recorded at a scan rate of 50 mV s^{-1} at different stages of the cycling experiment (solid line: cycle 10, broken line: cycle 60, dashed line: cycle 200 and dotted line: cycle 650) performed in the potential window 0/ −1.8 V in 1 M Et$_4$NBF$_4$–acetonitrile and corresponding to a discharge time of about 10 s.

capacitance loss is observed in all cases. This phenomenon is also illustrated by the evolution of the CVs upon cycling, recorded at 50 mV s^{-1} for poly(**1**) (Fig. 10). The evolution of the shape of the CVs is similar for all the polymers and is characterized by a gradual attenuation of the redox waves located at the most negative potentials. Thus, the capacitance loss after 650 cycles can be ranked in the following increasing order: poly(**1**) (−33%) ≈ poly(**9**) (−34%) < poly(**7**) (−39%) < poly(**2**) (−49%). This difference between the cyclability of the polymers might be explained as follows: i) the similar cyclability of poly(**1**) and poly(**9**) is attributed to the very similar structure of their corresponding monomers (*i.e.* the structure **1** is embeded in **9**); ii) the slightly lower cyclability of poly(**7**) could be due to the cyanobutadiene linkage between the two thiophene rings; iii) the poor cyclability of poly(**2**) may result from the destabilizing effect of the electron-donating methyl group on the negatively charged n-doped polymer. The poorer stability of poly(**7**) relative to poly(**1**) is presumably related to the reduction of the polymer double bond as previously reported for poly(dithienylethylene).[2a] On the other hand, the poorer stability of poly(**2**) compared to poly(**1**) is in agreement with our previous observations with electropolymerized polymers.[9]

Conclusion

A series of polymers were obtained from diaryl(cyanovinylene) monomers by chemical polymerization in the presence of an almost quantitative amount of FeCl$_3$ with an efficiency varying between 0 and 90%. The chemical composition of the polymers was evaluated by EDAX measurements and the presence of iron and/or chlorine, in some cases, was explained by the molecular structure of the monomer. The electrochemical properties of the polymers were investigated using composite electrodes and were in good agreement with the predictable effects of substitution patterns. Among the seven polymers that were studied, five have exhibited comparable or improved performance in comparison with other conducting polymers reported in the literature, with energy and power densities higher than 40 Wh kg^{-1} and 15 kW kg^{-1}. Therefore, the composite electrode technology used here appears to be suitable for obtaining high power densities since no important capacitance loss was observed for discharge times of about 10 s. This is in contrast with a previous report concerning composite polymer-based electrodes that were characterized by significant polarization behavior, which limited their energy and power capabilities.[13]

The highest performances were obtained with poly(**7**) and poly(**9**), which are derived from monomers with extended conjugation. A specific capacitance of 68 Ah kg^{-1} was reported for poly(**7**) in its n-doped state whereas a value of 90 Ah kg^{-1}

was found for poly(**9**) in its p-doped state. The performance of polymer-based supercapacitors was evaluated from cyclic voltammetry and galvanostatic charge/discharge experiments and the best results were achieved with poly(**9**) and poly(**7**)/ poly(**9**) assemblies that can deliver specific capacitances as high as 38 Ah kg^{-1} of polymer, specific energies of up to 75 Wh kg^{-1} and specific powers higher than 27 kW kg^{-1}. To our knowledge, this specific energy is the highest ever reported for conducting polymers used in capacitor configuration. Indeed, specific energies of 45 and 25 Wh kg^{-1} were recently reported for polythiophene derivatives[37c] and poly(1,5-di-aminoanthraquinone)[41]-based capacitors, respectively. More-over, a capacitor based on poly(**9**) was evaluated and was found to deliver energy and power densities of 68 Wh kg^{-1} and 24 kW kg^{-1} respectively, which are in good agreement with those predicted from experiments performed with single electrodes. Nevertheless, a capacitance loss of 45% has been observed after 1 300 cycles and was ascribed exclusively to the lack of cyclability of the n-doping process occurring at the negative electrode. In addition, cycling experiments were performed up to at least 650 cycles with single electrodes based on polymers of **1**, **2**, **7** and **9** in their n-doped state and capacitance losses ranging from 33 to 49%, depending on the polymer, were observed. These results were explained by the different molecular structures of the monomeric precursors, which affect the stability of the resulting polymers. Unfortunately, these capacitance losses are notably higher than that reported in the literature for another polythiophene derivative. Indeed, Ferraris *et al.*[37c] have recently reported a capacitance loss limited to about 10% after 1 000 cycles for poly[3-(3,4-difluorophenyl)thiophene] (MPFPT) electrodeposited on to carbon paper and cycled in its n-doped state in 0.2 M Et$_4$NBF$_4$–MeCN. We can postulate that the limited cyclability of the present series of polythiophene derivatives could be due to their particular cyanoethylene-type substructure. Other polymers are under investigations in our laboratory to evaluate the role of various groups.

References

1   J. Roncali, *Chem. Rev.*, 1997, **97**, 173; J. Roncali, *J. Mater. Chem.*, 1999, **9**, 1875.
2   G. Zotti, G. Schiavon and S. Zecchin, *Synth. Met.*, 1995, **72**, 275; G. Zotti, S. Zecchin, G. Schiavon, A. Berlin, G. Pagani and A. Canavesi, *Chem. Mater.*, 1997, **9**, 2940.
3   H. A. Ho, H. Brisset, P. Frère and J. Roncali, *J. Chem. Soc., Chem. Commun.*, 1995, 2309.
4   B. E. Conway, *Electrochemical Supercapacitors: Scientific Funda-mentals and Technological Applications*, Kluwer Academic/Plenum Publishers, New York, 1999.
5   P. Novak, K. Muller, K. S. V. Santanam and O. Hass, *Chem. Rev.*, 1997, **97**, 207; R. Kötz and M. Carlen, *Electrochim. Acta*, 2000, **45**, 2483.
6   M. Mastragostino, C. Arbizzani, R. Paraventi and A. Zanelli, *J. Electrochem. Soc.*, 2000, **147**, 407; M. Mastragostino, R. Paraventi and A. Zanelli, *J. Electrochem. Soc.*, 2000, **147**, 3167.
7   L. Li, C. Loveday, J. P. Ferraris and A. B. McEwen, in *Proc. Ninth Intl. Seminar on Double Layer Capacitors and Similar Energy Storage Devices*, ed. S. P. Wolsky and N. Marincic, Florida Educational Seminars Inc., Boca Raton, Fla., Dec. 1999.
8   E. Naudin, N. El-Mehdi, C. Soucy, L. Breau and D. Bélanger, *Chem. Mater.*, published on the web.
9   F. Fusalba, H. A. Ho, L. Breau and D. Bélanger, *Chem. Mater.*, 2000, **12**, 2581.
10 Q. T. Zhang and J. M. Tour, *J. Am. Chem. Soc.*, 1998, **120**, 5355.

11 R. Sugimoto, S. Takeda, H. G. Gu and K. Yoshino, *Chem. Express*, 1985, **1**, 635.
12 R. D. McCullough, *Adv. Mater.*, 1998, **10**, 93.
13 A. Laforgue, P. Simon, C. Sarrazin and J. F. Fauvarque, *J. Power Sources*, 1999, **80**, 142.
14 T. Sotomura, H. Uemachi, K. Takyeama, K. Naoi and N. Oyama, *Electrochim. Acta*, 1992, **37**, 1851; T. Sotomura, T. Tatsuma and N. Oyama, *J. Electrochem. Soc.*, 1996, **143**, 3152.
15 M. Lefebvre, Z. Qi, D. Rana and P. G. Pickup, *Chem. Mater.*, 1999, **11**, 262.
16 P. Soudan, H. A. Ho, L. Breau and D. Bélanger, in *Proc. Ninth Intl. Seminar on Double Layer Capacitors and Similar Energy Storage Devices*, ed. S. P. Wolsky and N. Marincic, Florida Educational Seminars Inc., Boca Raton, Fla., Dec. 1999.
17 P. Soudan, H. A. Ho, L. Breau and D. Bélanger, unpublished results.
18 B. P. Das and W. D. Boykin, *J. Med. Chem.*, 1973, **16**, 413; G. M. Badger, J. A. Elix and G. E. Lewis, *Aust. J. Chem.*, 1965, **18**, 70.
19 A. Elkassmi, G. Heraud, W. Büchner, F. Fache and M. Lemaire, *J. Mol. Catal.*, 1992, **72**, 299.
20 E. Jones and I. M. Moodie, *Tetrahedron*, 1965, **21**, 2413.
21 X. Wu, T. A. Chen and R. D. Rieke, *Macromolecules*, 1995, **28**, 2101; X. Wu, T. A. Chen, R. D. Chen and R. D. Rieke, *Tetrahedron Lett.*, 1994, **35**, 3673.
22 L. H. Klemm and K. W. Gopinath, *J. Heterocycl. Chem.*, 1965, **2**, 225.
23 J. Nakayama, S. Murabayashi and M. Hoshino, *Heterocycles*, 1986, **24**, 2639.
24 T. B. Patrick and J. L. Honneger, *J. Org. Chem.*, 1974, **39**, 3791.
25 G. Alberghina, M. E. Amato, A. Corsaro, S. Fisichella and G. Scarlata, *J. Chem. Soc., Perkin Trans. 2*, 1985, 353.
26 M. S. A. Abdou, X. Lu, Z. W. Xie, F. Orfino, M. J. Deen and S. Holdcroft, *Chem. Mater.*, 1995, **7**, 631.
27 J. Rault-Berthelot, C. Rozé, M. M. Granger and E. Raoult, *J. Electroanal. Chem.*, 1999, **466**, 144; J. Rault-Berthelot, M. M. Granger and E. Raoult, *J. Electroanal. Chem.*, 2000, **486**, 40.
28 B. Fabre, P. Marrec and J. Simonet, *J. Electrochem. Soc.*, 1998, **145**, 4110.
29 Z. Qi and P. G. Pickup, *J. Chem. Soc., Chem. Commun.*, 1992, 1675.
30 Z. Qi and P. G. Pickup, *Anal. Chem.*, 1993, **65**, 696.
31 Z. Qi, N. G. Rees and P. G. Pickup, *Chem. Mater.*, 1996, **8**, 701.
32 P. Soudan, P. Lucas, L. Breau and D. Bélanger, *Langmuir*, 2000, **16**, 4362.
33 P. Bauerle, K.-U. Gaudl, F. Würthner, N. S. Sariciftci, H. Neugebauer, M. Mehring, C. Zhong and K. Doblhofer, *Adv. Mater.*, 1990, **2**, 490.
34 K. Nishio, M. Fujimoto, N. Yoshinaga, O. Ando, H. Ono and T. Suzuki, *J. Power Sources*, 1991, **34**, 153.
35 A. Rudge, I. Raistrick, S. Gottesfeld and J. P. Ferraris, *Electrochim. Acta*, 1994, **39**, 273; A. Rudge, J. Davey, I. Raistrick, S. Gottesfeld and J. P. Ferraris, *J. Power Sources*, 1994, **47**, 89.
36 G. Zotti and G. Schiavon, *Synth. Met.*, 1994, **63**, 53.
37 D. J. Guerrero, X. Ren and J. P. Ferraris, *Chem. Mater.*, 1994, **6**, 1437; J. P. Ferraris, M. M. Eissa, I. D. Brotherson, D. C. Loveday and A. A. Moxey, *J. Electroanal. Chem.*, 1998, **57**, 459; J. P. Ferraris, M. M. Eissa, I. D. Brotherson and D. C. Loveday, *Chem. Mater.*, 1998, **10**, 3528.
38 H. Sarker, Y. Gofer, J. G. Killian, T. O. Poehler and P. C. Searson, *Synth. Met.*, 1997, **88**, 179; Y. Gofer, J. G. Killian, H. Sarker, T. O. Poehler and P. C. Searson, *J. Electroanal. Chem.*, 1998, **103**, 443; J. G. Killian, Y. Gofer, H. Sarker, T. O. Poehler and P. C. Searson, *Chem. Mater.*, 1999, **11**, 1075.
39 Y. Wei, C. C. Chan, J. Tian, G. W. Jang and K. F. Hsueh, *Chem. Mater.*, 1991, **3**, 888.
40 G. Barbarella, L. Favaretto, M. Zambianchi, O. Pudova, C. Arbizzani, A. Bongini and M. Mastragostino, *Adv. Mater.*, 1998, **10**, 551.
41 K. Naoi, S. Suematsu and A. Manago, *J. Electrochem. Soc.*, 2000, **147**, 420.